RSC Advances

ROYAL SOCIETY OF CHEMISTRY

www.rsc.org/advances

MCR-ALS as an effective tool for monitoring subsequent phase transitions in pure and doped DPPC liposomes

Katarzyna Cieślik-Boczula[1*], Bogusława Czarnik–Matusewicz[1], Margarita Perevozkina[2] and Maria Rospenk[1]

[1]Faculty of Chemistry, University of Wroclaw, F. Joliot-Curie 14, 50-383 Wroclaw

[2]Tyumen State Agricultural Academy, 625003 Tyumen, Republic 7, Russian Federation

* Corresponding author: Katarzyna Cieślik-Boczula,

Faculty of Chemistry, University of Wroclaw,

ul. F. Joliot-Curie 14, 50-383 Wrocław, Poland

Tel.: +48 71 375 7209; fax: +48 71 328 2348.

E-mail address: katarzyna.cieslik@chem.uni.wroc.pl

Abstract

The MCR-ALS method was applied to increase the structural informations derived from infrared spectra of pure and doped dipalmitoylphosphatidylcholine (DPPC) liposomes. Pure DPPC vesicles and mixed ones with long-chain homologues of the phenol substituted by a tert-butyl moiety were investigated using the attenuated total reflectance Fourier-transfer infrared spectroscopy (FTIR-ATR). A combination of pure spectral profiles with pure concentration ones, which were derived from MCR-ALS calculations, enabled us to discuss in detail the structural characteristics of each pure phase state, which occur during a heating of pure as well as mixed lipid systems. Additionally, alterations of relative concentrations of subsequent components, which were represented by different pure phase states, associated with individual phase transitions, were determined in both pure and mixed DPPC systems. As far as we known, it is the first application of the MCR-ALS calculation in analysis of FTIR-ATR spectra of DPPC membranes.

Keywords

Multivariate curve resolution-alternating least squares method (MCR-ALS), attenuated total reflectance Fourier-transfer infrared spectroscopy (FTIR-ATR), DPPC liposomes, phase transition

Abbreviations

DPPC – 1,2-Dipalmitoyl-sn-glycero-3-phosphocholine**,** MCR-ALS – Multivariate curve resolution-alternating least squares method, FTIR-ATR – attenuated total reflectance Fourier-transfer infrared spectroscopy, Tm – main phase transition, Tp – pre-transition

1. Introduction

The structure and physicochemical properties of different lipid systems have been studied using numerous methods such as DSC, X-ray, EPR, NMR, and fluorescence spectroscopy [1-4]. The attenuated total reflectance Fourier-transfer infrared spectroscopy (FTIR-ATR), too, has widely been used to investigate lipid membranes [5-8]. The FTIR spectroscopy offers a possibility to observe alterations of vibration frequencies, which are characteristic for lipid groups in different parts of a molecule, and therefore various regions of a lipid bilayer could be monitored simultaneously in one experiment. The FTIR spectroscopy can thus provide a detailed insight into a structure of a lipid bilayer, but the analysis of FTIR spectra is not straightforward. Data processing is necessary to extract the descriptive chemical information from spectra complicated by overlapping vibrational bands. The most common method, which enables a more precise determination of peak location in infrared spectra of lipid membranes is one-dimensional (1D) analysis accompanied by the second derivative, the Fourier self-deconvolution or by the curve fitting methods. More recently much efficient analysis, such as two-dimensional correlation spectroscopy (2DCOS) has been involved to elucidate molecular dynamics as well as intra- and intermolecular structural correlations in lipid bilayers [9-13]. As far as we know, this paper presents the first application of the multivariate curve resolution-alternating least squares (MCR-ALS) method of analysis of FTIR-ATR spectra of biomembrane lipid systems in detection and characterization of structures of phase states of pure and doped DPPC membranes. It should be mentioned that there are a few articles in which MCR-ALS analysis is applied with a success to infrared spectra of lipid systems, mainly associated with oil molecules. For example, MCR-ALS calculations facilitate monitoring the aging of oils accompanied mostly by a lipid oxidation [14-16], and this method executes characterization of reactions associated with oil molecules [17]. Additionally, MCR-ALS is an effective tool to state a molecular composition of organic

aggregates including biomolecules of proteins, carbohydrates and lipids [18]. The quantification of the main types of lipids in living cells can also be done [19]. Nevertheless, all literatures, which we were able to find, were dedicated to other classes of lipids than lipids of biological membranes. Lipids of biomembranes because of their huge biological functions should be considered as a separate task of many scientific studies. Biomembrane lipids have characteristic properties such as thermotropic and lyotropic phase transitions, which determine the most important biological functions of cell membranes (e.g. transport across the membrane, its permeability, activity of membrane proteins etc.). Understanding lipid phase transition processes can help to resolve membrane-dependent mechanisms of most biological processes. DPPC liposomes are commonly used in many scientific laboratories for studying processes associated with phase transitions and/or states of a lipid membrane below and above the transition temperature [7,20]. The DPPC lipid is one of the most numerous members of the phosphatidylcholine (PC) group, which is the most prevalent lipid group among those constituting the basic structure of eukaryotic cell membranes [21]. In pure DPPC bilayers during the heating process at least two phase transitions can be observed: the pre-transition (Tp) and the main phase transition (Tm) with three phase states differ in a hydration level, mobility of lipids molecules, as well as in a lateral chain packing and conformation of hydrophobic and hydrophilic groups of DPPC molecules. Using the MCR-ALS method in the analysis of FTIR spectra of DPPC membranes allowed us to clearly characterize structural changes in the pure phase states before and after the main phase transition, as well as around more problematic pre-transition. The pre-transition is associated mainly with structural changes in a polar region of a lipid bilayer. Unfortunately, many vibrational bands, which are sensitive to this process overlap one another, and their analysis is very often complicated and obscure. The MCR-ALS method applied to the low-frequency region of DPPC liposomes enabled us to overcome the mentioned above difficulties. The temperature of Tp was clearly

appointed, and a structural character of both phase states before and after Tp of DPPC membranes was described in detail. Furthermore, the effect of biologically active compounds with a long hydrocarbon chain – ICPANs – on the hydrophobic and hydrophilic regions of doped DPPC membranes were investigated in detail using the FTIR-ATR spectroscopy supported by the MCR-ALS analysis. MCR-ALS can also give rise to an high-resolution increase in data of doped lipid systems. ICPANs are synthetic molecules, which can control a plant cell growth [22]. They have an influence on activities of proteins [23] and work as an effective antioxidant in membranes [24-26]. Additionally, the oxidation of lipids derived from a homogenized mouse brain is inhibited by the presence of ICPANs and depends on the length of their hydrocarbon chain [25]. The most efficient antioxidants are the homologues from C8 to C12 [25,27,28]. As amphiphilic molecules they can strongly interact with lipid membranes, which is responsible for most of their biological functions. It was stated, that interactions between ICPANs and lipid bilayers strongly depend on the number of carbon atoms in the acyl tail of ICPAN [9,29].

The aim of presented paper was to show the utility of the MCR-ALS method on the basis of structural analysis of pure as well as ICPAN-mixed DPPC membranes as a function of increased temperature, which were studied using FTIR-ATR spectroscopy. The biggest advantage of applying MCR-ALS method to the DPPC membranes is associated with presentation of concentration profiles. These curves show an evolution of changes in relatives concentrations of each pure phase state present in lipid membranes during the heating. Such lines obtained from conventional methods of analysis, such as curve-fitting, will be disturbed by unsteady fitting, which should be performed on many sub-bands [30,31]. It is well known that the de-convolution process is sensitive to a number of sub-components. A high number of sub-components seriously obscures real results, and in such case a good de-convolution curve can be represented by completely different sub-bends. This not reliable and time-consuming

conventional method can be thus easily replaced by chemometric (MCR-ALS) analysis. Using MCR-ALS method can increase the structural information about our systems, and finally it can deepen the knowledge of the mechanism of membrane-mediated biological activities of ICPAN molecules. ICPANs can develop some of their biological effects by modulation of a membrane structure.

2. Experimental section

2.1. Materials

1,2-Dipalmitoyl-sn-glycero-3-phosphocholine (DPPC) with a purity of > 99.8% was obtained from Sigma-Aldrich, Germany, and was used without further purification. ICPAN-C8 ((N,N-dimethyl-N-octyl-2-ammonioethyl)-3-(3,5-di-tert-butyl-4-hydroxyphenyl) propionate bromide), ICPAN-C10 ((N,N-dimethyl-N-decyl-2-ammonioethyl)-3-(3,5-di-tert-butyl-4-hydroxyphenyl) propionate bromide), ICPAN-C12 ((N,N-dimethyl-N-dodecyl-2-ammonioethyl)-3-(3,5-di-tert-butyl-4-hydroxyphenyl) propionate bromide) and ICPAN-C16 ((N,N-dimethyl-N-hexadecyl-2-ammonioethyl)-3-(3,5-di-tert-butyl-4-hydroxyphenyl) propionate bromide) were synthesized by a known procedure [23] at the Institute of Biochemical Physics of the Russian Academy of Sciences, Moscow, Russia. Schematic representation of the ICPAN structure is presented in **Figure 1**.

2.2. FTIR-ATR measurement

10 mg of DPPC and adequate amount of ICPANs (30 mol%) were dissolved in chloroform and then dried under a stream of nitrogen. Dry ICPAN/lipid films were hydrated by addition of 10 mM phosphate buffer, pH 7.2 during 10 of the heating/cooling cycles. The ICPAN/DPPC suspensions were recorded on a ZnSe-ATR crystal with a Nicolet Magna 860 FTIR spectrometer equipped with a Globar source, a KBr beam splitter and a DTGS detector. The 128 scans with a resolution of 2 cm^{-1} were applied. The spectra were recorded during

heating from 5 to 60 °C with an interval of 5 °C, and 2.5 °C, at near the temperature of phase transition. At each temperature a sample was equilibrated for 5 min before acquisition of a spectrum. A water-bath circulator (Julabo Labortechnik GmbH) was used to control a temperature.

2.3. Pretreatment of the FTIR-ATR data

Before the MCR-ALS analysis of the FTIR-ATR spectra of pure and ICPAN-mixed DPPC samples the following treatment steps were applied: subtraction of a buffer spectrum from a spectrum of sample dispersion, separation on two spectral ranges: 2970-2825 cm^{-1} (high-frequency region) and 1505-940 cm^{-1} (low-frequency region), and a noise reduction by a Fourier smoothing. This pretreatment of data was accomplished by GRAMS/32 AI (6.0) software (Galactic Industries Corporation). Normalization over the integral area and MCR-ALS analysis were carried out in Matlab 6.5 software. MCR-ALS algorithm was implemented as the Matlab-code by Roma Tauler and Anna de Juan, the University of Barcelona (http://www.mcrals.info/) [32].

2.3.1. MCR-ALS: principles and algorithm

The FTIR-ATR spectra recorded during a particular experiment after pretreatment were arranged in a data matrix, **D**. For each sample, *i.e.* pure and ICPAN-mixed DPPC samples, three separate data matrices were generated, $\mathbf{D_1}$, $\mathbf{D_2}$ and $\mathbf{D_c}$. $\mathbf{D_c}$ matrix is complete data matrix, which contains in rows experimental spectra in the whole-frequency range, $\mathbf{D_1}$ as the low-frequency portion of the data matrix contains in rows the low-frequency range of measured spectra, and $\mathbf{D_2}$ is the high-frequency portion of the data matrix. The dimension of each matrix was *Nr* rows x λm columns, where *Nr* is the number of spectra recorded at successive temperatures, and λm is the number of wavenumbers measured. MCR-ALS was applied to analyze separately the $\mathbf{D_1}$, $\mathbf{D_2}$ and $\mathbf{D_c}$ matrices. The decomposition of the experimental data matrix **D** was according to the equation:

$$\mathbf{D} = \mathbf{C}\mathbf{S}^{\mathbf{T}} + \mathbf{E} \qquad (1)$$

where **C** and $\mathbf{S}^{\mathbf{T}}$ are, respectively, the matrix of the calculated pure concentration profiles, and the matrix of calculated pure spectral profiles for each of the species present in the system. **E** is the residual error matrix between **D** and a model $\mathbf{C}\mathbf{S}^{\mathbf{T}}$. In order to find initial estimates for MCR-ALS calculation, the evolving factor analysis (EFA) was applied for the evolving profiles in the domain of the temperatures. The interactive least square calculation of **C** and $\mathbf{S}^{\mathbf{T}}$ was performed in a constrained condition. Constrains help to minimize/overcome rotational ambiguity and was played to **C** or $\mathbf{S}^{\mathbf{T}}$ in every step of interaction. In our studies the concentration and spectral profiles were forced to be positive using the non-negativity constrain. Additionally, only one maximum in concentration profiles was applied by the unimodality constrain. For MCR-ALS fittings the number of interactions was between 9 and 30, standard deviation of residuals vs. experimental data was 0.0002 ± 0.0001, percent of variance explained was 99.99 ± 0.05, fitting error (lack of fit, lof) in % (PCA) 0.015 ± 0.01, and fitting error (lack of fit, lof) in % (exp) 0.98 ± 0.7.

Each sample was prepared three times, the temperatures of both phase transitions present in all systems were stable, Tm and Tp derived from each MCR-ALS analysis differ by the value of ± 0.30 °C.

3. Results and discussion

The main objectives of MCR-ALS with EFA analysis are the isolation, resolution, and relative quantification of the main sources of variation in a particular data set. The MCR-ALS method performs the bilinear decomposition of a measured system into separate components. It needs the chemical assumption about the contribution of the different components in a system under examination.

In the EFA analysis, singular values, which are square roots of eigenvalues, are calculated by using singular values decomposition of 1, 2, 3, …, *n* rows of the data matrix **D** (forward curve) and from the opposite direction *n*-1, *n*-2, …, 1 rows (backward curve). The intersects of corresponding forward and backward curves demonstrate the number of species, which independently contribute to a measured signal. The EFA calculation gives initial estimations of the concentration profiles according to estimated numbers of independent components, and they are used to start the iterative process in the MCR-ALS procedure. Physically meaningful set of concentration and spectral profiles is calculated using the constrained alternating least-squares (ALS) optimization.

3.1. MCR-ALS analysis of the pure DPPC liposomes

EFA calculations were performed independently on $\mathbf{D_1}$, $\mathbf{D_2}$ and $\mathbf{D_c}$ matrices, each of them was composed of one of three regions of FTIR spectra of the pure DPPC liposomes. In each case of calculations, two principal singular values were obtained in the forward and backward analyses, see **Figure 2A.** Thus, two components, represented by different phase states of the DPPC bilayer, independently contributed to measured signals when the low-, high-, and whole-frequency regions were separately analyzed. **Figure 2B, C** represents graphs of concentration and spectral profiles for detected phase processes in the DPPC bilayer, which were obtained from the MCR-ALS calculations with suitable constraints.

Figure 1

Figure 2

The high-frequency range (2970 - 2825 cm^{-1}) of infrared spectra of DPPC membranes is represented by bands of antysymmetric and symmetric stretching vibrations of CH_2 groups ($\nu_{as,s}(CH_2)$) of lipid hydrocarbon chains. Spectral parameters of the $\nu_{as,s}(CH_2)$ bands monitor the alterations of the ratio of trans to gauche conformers of lipid CH_2 moieties. When the $\nu_{as,s}(CH_2)$ region of heated DPPC liposomes was tested by MCR-ALS, the curves of the relative concentration of the low- and high-temperature components crossed each other at the point of temperature of the chain-melting main phase transition (Tm = 41 °C), see **Figure 2B** (solid lines). A shape of concentration profiles reflected a character of an decrease in a relative concentration of the pure low-temperature phase and a nature of an increase in a contribution of the pure high-temperature state of the DPPC bilayer during an rise in temperature. Infrared spectroscopy is an excellent tool to monitor the main phase transition in lipid bilayers [5,7]. A simple analysis, based on a shift of a maximum position of the $\nu_{as,s}(CH_2)$ bands, shows a sharp jump of the melting curve at the temperature of Tm. Using the MCR-ALS method in analysis of the high-frequency region of heated DPPC liposomes allowed us to characterize this process in a deeper way. The evolution of the relative concentration of the pure gel and the pure liquid-crystalline phases was depicted. Additionally, the spectra of each pure lipid phase can be derived from this analysis. The pure spectral profile associated with the low-temperature component showed the $\nu_{as,s}(CH_2)$ bands with the maximum positions at 2917 and 2850 cm^{-1}, respectively, characteristic for the trans-rich pure gel phase state of the DPPC bilayer, see **Figure 2C** (solid line). In addition, the pure spectral profile for the second component indicated a blue shift of the $\nu_{as,s}(CH_2)$ bands to the 2922 and 2853 cm^{-1} positions, respectively. The high-temperature component adopts therefore the conformationally disordered gauche-rich pure fluid state of lipid membranes. Furthermore, the MCR-ALS analysis performed on a whole-frequency range of FTIR spectra of DPPC liposomes appointed a value of Tm as a consequence of domination of the transition

from the trans-rich low-temperature gel phase to the gauche-riche high-temperature lipid-crystalline state, see **Figure 2B** (dashed lines).

Interestingly, when the low-frequency data matrix was investigated, the intersection of both the low- and the high-temperature concentration profiles pointed the temperature 33 °C, which is characteristic for the pre-transition (Tp) of the DPPC bilayer, see **Figure 2B** (dashed-two dotted lines). A good correlation between the temperature of Tp derived from the DSC measurement for DPPC liposomes [33] and this temperature assigned from the intersection of the two lines for the low- and high-temperature components (derived from MCR-ALS calculation) was a rationale for selecting this method to determine the temperature of phase transition during the analysis of low-frequency region. The transition from the gel phase (L'_β) to the rippled gel phase (P'_β), called pre-transition, is accompanied by an increase in rotational and conformational movements mainly of polar lipid groups [34,5]. Additionally, the hydration of the DPPC bilayer rises during Tp [35,36]. Bands for vibrations of lipid polar moieties such as phosphate, carbonyl and choline groups dominate in the low-frequency range (1505 - 940 cm^{-1}) of DPPC spectra: see **Figure 2C** for band assignment. The MCR-ALS calculation performed on the low-frequency part of spectra under study was therefore able to describe the phenomena of the pre-transition of the DPPC bilayer, while the high-frequency vibrational region, which is represented mainly by the stretching vibrations of the lipid hydrocarbon CH_2 groups, described the main phase transition. Pure phase states before and after Tp of DPPC membranes were characterized by spectral changes in ν_{as}(C-O-C), $\nu_s(PO_2^-)$, ν(C-O-P-O-C), and ν(CO-O-C) bands, see **Figure 2C**. It is a consequence of structural rearrangements and alterations of interactions of polar head-group moieties, which take place during Tp [5, 34-36]. Additionally, the thesis that the conformational membrane fluidization (i.e. trans to gauche isomerization) starts already at Tp [37], was confirmed in our studies by a decrease in the $\delta(CH_2)$ band intensity and by a low-frequency shift of its maximum; compare

the low-temperature spectral profile with the high-one of the low-frequency region in **Figure 2C**. Such spectral changes in the $\delta(CH_2)$ band are characteristic for the trans-gauche-associated disturbance of lateral packing of lipid chains. Furthermore, the spectral variations in the 1350 – 1200 cm^{-1} vibrational region were associated with the disappearance of CH_2 wagging vibration bands progression ($\omega(CH_2)$) of all-trans segments, as a result of an increase in population of the gauche conformers of DPPC chains [37]. A vanish of $\omega(CH_2)$ bands revealed at the high-temperature phase the $\nu_{as}(PO_2^-)$ band, which position was non-perturbed by a temperature increase [38,39].

The pre-transition involves a smaller change in a structure of DPPC bilayers and therefore induces more subtle alterations in an infrared spectrum than the main transition. For this reason, a detection of Tp in the DPPC bilayer using infrared spectroscopy is not an easy task [34]. Application of the MCR-ALS analysis to series of FTIR-ATR spectra of DPPC liposomes allowed us to increase the resolution of spectra under study, and finally we were able to obtain more structural informations about the system. The concentration profiles derived from MCR-ALS analysis therefore clearly pointed the temperature of Tp, generally poorly visible in IR spectra. Additionally, this method allowed us to separate pure phases, which take place below and above of Tp during the heating of the DPPC bilayer, and to show the evolution of changes of their relative concentrations.

3.1.1. Sensitivity of MCR-ALS data to changes in input parameters

The effect of variations in a number, a length of the spectra and their smoothing was tested in order to show the sensitivity of MCR-ALS results to changes in input parameters. The reduction in a number of the analyzed spectra of DPPC liposomes in both the low- and the high-frequency regions form 15 even to 9, allowed us to obtain still suitable results, see **Figure 3 and 4** for concentration and spectral profiles, respectively. For study this effect, the first three spectra and the last three spectra were eliminated from the MCR-ALS calculations.

Execution of the MCR-ALS analysis on non-smoothing spectra also gave quite similar results to these for Fourier smoothed data. Additionally, an increase in the length of studied spectra was not able to disturb seriously the final results. The temperatures of Tm and Tp of DPPC liposomes derived from MCR-ALS analysis with different input parameters differed maximum by ± 1.4 °C, see **Figure 3**. Spectral profiles of the high-temperature component derived from MCR-ALS analysis of the high-frequency range and spectral profiles of the low-temperature component calculated for the low-frequency range revealed some sensitivity to alterations in input spectra. On the other hand, the low- and high-temperature components obtained from analysis of the high- and low-frequency ranges, respectively, were almost unperturbed, see **Figure 4**. It can be concluded that in each case MCR-ALS results give similar physical descriptions of phase transition phenomena present in the DPPC liposomes during the heating. The temperatures of Tm and Tp are similar to these obtained from other experiments [3,5,33], and spectral profiles characterize the structure of pure phase states in agreement with literature data [5,7,31,34-39]. Additionally, the evolution of relative concentrations of the low- and high-temperature phase states, which is one of the most important additional informations derived from MCR-ALS analysis, is not meaningfully disturbed by changes in input data parameters, see **Figure 3**.

Figure 3

Figure 4

3.2. MCR-ALS analysis of the ICPAN-DPPC mixtures

3.2.1. Pure concentration profiles

MCR-ALS analysis can be also applied to doped DPPC membranes. In this case, pure phase states can be separated and characterized too.

EFA calculation, which was applied to the low-, high- or whole-frequency regions of each ICPAN/DPPC mixture, produced two forward-backward principal component values for each frequency range. In all ICPAN-mixed liposomes two phase transitions were thus detected, similarly to those received in the pure DPPC liposomes. One of these transitions was accompanied by the trans-gauche isomerization of hydrocarbon chains, and the second was connected with changes in a hydrophilic part of ICPAN-DPPC mixtures. The graphical representation of intersections of the concentration profiles of the low- and high-temperature components for the low-, high-, and whole-frequency regions is presented in **Figure 5**. They appointed temperatures of phase transitions accompanied by changes in hydrophilic or in hydrophobic parts of ICPAN-mixed DPPC samples.

Figure 5

All DPPC systems doped with ICPAN molecules with a different length of the hydrocarbon chain showed different behavior of the concentration profiles as a function of temperature, compared with that for the pure DPPC liposomes; see **Figures 2B** and **5**. The temperatures of phase transitions, triggered by structural alterations in both polar and apolar regions of ICPAN-DPPC systems, were clearly lower compared with Tp and Tm of the pure DPPC liposomes, respectively. Additionally, a characteristic order of structural changes during the heating of pure DPPC membranes, that is at first in the hydrophilic region and then in the hydrophobic one, was not retained in the presence of ICPAN compounds, see **Figure 5**.

In case of ICPAN homologues with the C8, C10, and C16 alkyl chain lengths, when the high- and whole-frequency regions were analyzed, the intersections of concentration profiles of the low- and high-temperature phases appeared at lower temperatures than the cross point of the high- and the low-temperature concentration profiles derived from MCR-ALS calculations of the low-frequency region. Only in case of ICPAN-C12 these three cross-points were almost at the same temperature, see **Figure 5D**. Thus, during the heating process of DPPC liposomes doped with C8, C10 and C16 homologues, an increase in gauche conformers of hydrocarbon chains appeared as the first, and then, after few $^{\circ}$C, the structural alterations in the hydrophilic region came out. This sequence is in an opposite order to one observed in the pure DPPC membranes. Interestingly, in the ICPAN-C12-DPPC mixture the structural changes in both regions took place simultaneously. The temperature of conformational fluidization of hydrocarbon chains decreases with an increase in the number of carbon atoms of the ICPAN alkyl tail, i.e. in the order of C8 > C10 > C16. Temperatures of the trans-gauche-chain-melting phase transitions for all systems under study varied from 24 to 15 °C, which was about 26 – 17 °C lower than Tm of the pure DPPC liposomes. Interestingly, the phase transition temperature, triggered by alterations of polar groups, decreased to nearly the same temperature (25 ± 2 °C) in all ICPAN-DPPC mixtures. This temperature down-shift in relation to Tp of pure DPPC is thus clearly smaller than in case of the temperature reduction of chain-melting phase transition of ICPAN-mixed DPPC samples in comparison with Tm of pure DPPC.

Similarly to pure DPPC liposomes, the MCR-ALS analysis performed on the whole frequency range of FTIR spectra of ICPAN-mixed DPPC samples also showed a domination of the chain-meting transition accompanied by trans-gauche isomerization on the transition derived from polar lipid group rearrangements.

3.2.2. Pure spectral profiles

The pure spectral profiles were generated for each low- and high-temperature component in the MCR-ALS analysis. The high- and the low-frequency spectra attributed to the low- and the high-temperature phase states of ICPAN-DPPC mixtures are depicted in **Figure 6.** They allowed us to characterize separately the structure of polar and apolar parts of ICPAN-DPPC aggregates in the pure low- and pure high-temperature phase states.

The high-frequency range analyzed using the MCR-ALS method was represented by the $\nu_{as,s}(CH_2)$ bands, which are commonly accepted vibrational indicators sensitive to trans-gauche isomerization of hydrocarbon chains. The blue shift of the maximum position of $\nu_{as,s}(CH_2)$ bands, an increase in their half-width, and a decrease in the band intensity are generally recognized as a grow in the population of gauche conformers. The maximum positions of $\nu_{as,s}(CH_2)$ bands and their half-widths for all ICPAN-DPPC samples under study are collected in **Table 1.** The presence of ICPAN homologues in DPPC membranes shifted the maxima of $\nu_{as,s}(CH_2)$ bands to higher frequencies and raised their half-widths, as a consequence of an increase in the contribution of gauche conformers in the hydrophobic region of ICPAN-DPPC mixtures. These changes were characteristic for both the low- and the high-temperature phase states. Additionally, the biggest differences in spectral parameters of $\nu_{as,s}(CH_2)$ bands were observed between the pure and ICPAN-C12-doped DPPC samples. Thus, the ICPAN-C12-DPPC mixture, which as the only one showed structural rearrangements of hydrophobic and hydrophilic regions at the same temperature, had the highest conformational fluidization of the hydrocarbon chain region in both the pure high- and the pure low-temperature phase states.

Figure 6

Table 1

The MCR-ALS analysis of $\delta(^{+}N(CH_3)_3)$, $\nu_{as,s}(PO_2^-)$, ν(C-O-P-O-C), and ν(CO-O-C) bands, which are present in the low-frequency range (see **Figure 6)**, showed the structural rearrangements of polar lipid moieties in ICPAN-DPPC mixtures. A comparison of a structure of hydrophilic region between pure phases of DPPC membranes mixed with different ICPAN homologues, and an illustration of the effect of an increase in temperature, were possible on the basis of analysis of the low-frequency pure spectral profiles.

All ICPAN molecules significantly altered the intensity of the $\delta_{sym}(^{+}N(CH_3)_3)$ band centered at approximately 1400 cm^{-1}. A similar increase in intensity of this band in relation to the intensity of the $\delta_{sym}(^{+}N(CH_3)_3)$ band of the pure DPPC system, was observed for mixtures with ICPAN-C8, -C10, and -C12. This effect was present in both before and after Tp phase states. On the other hand, the C16 homologue induced a decrease in the $\delta_{sym}(^{+}N(CH_3)_3)$ band intensity. The state of lipid choline groups in the presence of all of ICPANs is thus different form that in the pure DPPC membrane, and it is not remarkably affected by a temperature growth.

The $\nu_{as}(PO_2^-)$ band is a very sensitive vibrational indicator of a level of lipid bilayer hydration. In a dry DPPC state this band has a maximum at approximately 1260 cm^{-1}, whereas in a fully hydration condition it reaches the position of 1220 cm^{-1} [40]. Additionally, the position of this band does not depend on the lipid phase state [38]. In low- and high-temperature phase states for all ICPAN-DPPC systems, the phosphate groups of DPPC molecules were in a similar fully-hydrated state, because the maximum of the $\nu_{as}(PO_2^-)$ band was always located at similar position, i.e. at 1223 cm^{-1}, see **Figure 6.** On the other hand, the conformational rearrangement of lipid phosphate groups and CO-O-C, C-O-P-O-C regions were affected by ICPAN molecules. In the pure DPPC liposomes, $\nu_s(PO_2^-)$, ν(CO-O-C) and

ν(C-O-P-O-C) vibrations gave rise to the band with the maximum at near 1077 cm^{-1}. In the state above Tp, incorporation of each ICPAN homologue caused splitting of this one band into two subbands, which are centered at 1084 and 1065 cm^{-1}. On the other hand, one band at 1077 cm^{-1} was still present in the low-temperature phase of DPPC samples mixed with the C8, C10 and C12 homologues. The transition from the low-temperature phase to the high-one was thus accompanied by the splitting of this band. The exception was the ICPAN-C16-DPPC mixture, where two subbands were present in the whole-temperature range. The reorientation and interaction of lipid phosphate groups and CO-O-C, C-O-P-O-C regions are thus differently influenced by the presence of ICPAN molecules with a different alkyl chain length of ICPAN molecules and by an increase in temperature of systems under study.

4. Conclusions

Results presented in this manuscript reveal a high sensitivity of the MCR-ALS method on structural changes developed during the subsequent phase transitions in the pure and ICPAN-doped DPPC liposomes. MCR-ALS data could be correlated in a direct manner with alterations of interactions and rearrangements of different lipid groups. Detailed description, which part of the system is responsible for the particular transition, is thus allowed. MCR-ALS analysis generates the infrared spectrum for each pure phase associated with individual phase transitions. Additionally, the changes of relative concentrations of each pure phase are graphically shown. Application of the MCR-ALS calculations to the infrared spectra of membrane lipid systems increases thus significantly structural informations about measured systems through isolation and relative quantification of pure components.

Both the pure spectral and the pure concentration profiles confirmed that a structure of the lipid bilayer is substantially perturbed in all ICPAN-DPPC systems under study. In pure DPPC liposomes as well as in the ICPAN-mixed DPPC mixtures two phase transitions are

detected by MCR-ALS analysis of FTIR-ATR spectra. These transition processes, which were developed in hydrophobic or hydrophilic parts of systems under study, occur in a different order depending on the chain length of incorporated ICPANs. One of these transitions is always accompanied with conformational fluidization derived from an increase in population of gauche conformers in hydrocarbon chains. In the next phase transition, structural changes of hydrophilic regions take place.

Acknowledgements

This work was supported by the Foundation for Polish Science - the programme POMOST, co-financed by the European Union within European Regional Development Fund (V edition, 2012) and by the grant nr DEC-2012/05/B/ST4/02029 (OPUS) from the National Science Centre. We thank the ÖAD (project nr. PL 07/2013) for additional financial support.

References

[1] K. Cieślik-Boczula, R. Petrus, G. Köhler, T. Lis and A. Koll, *J. Phys. Chem. B* 2013, **117**, 2938.

[2] K. Cieślik-Boczula, S., Küpcü, D. Rünzler, A. Koll and G. Köhler, *J. Mol. Struct.* 2009, **919**, 373.

[3] K. Cieślik-Boczula and A. Koll, *Biophys. Chem.* 2009, **140**, 51.

[4]D. Pentak, *Thermochim. Acta* 2014, **584**, 36.

[5] H. L. Casal and H. H. Mantsch, *Biochim. Biophys. Acta* 1984, **779**, 381.

[6] D. G. Cameron, H. L. Casal, E. F. Gudgin and H. H. Mantsch, *Biochim. Biophys. Acta* 1980, **596**, 463.

[7] K. Cieslik-Boczula, J. Szwed, A. Jaszczyszyn, K. Gasiorowski and A. Koll, *J. Phys. Chem. B* 2009, **113**, 15495.

[8] K. Cieślik-Boczula, J. Maniewska, G. Grynkiewicz, W. Szeja, A. Koll and A.B. Hendrich, *Vib. Spectrosc.* 2012, **62**, 64.

[9] M. Murawska, K. Cieślik-Boczula and B. Czarnik-Matusewicz, *J. Mol. Struct.* 2010, **974**, 183.

[10] J. Szwed, K. Cieslik-Boczula, B. Czarnik-Matusewicz, A. Jaszczyszyn, K. Gasiorowski, P. Swiatek and W. Malinka, *J. Mol. Struct.* 2010, **974**, 192.

[11] V. Volkov and P. Hamm, *Biophys. J.* 2004, **87**, 4213.

[12] V. V. Volkov, R. Chelli,, W. Zhuang, F. Nuti, Y. Takaoka, A. M. Papini. S. Mukamel and R. Righini, *PNAS* 2007, **104**, 15323.

[13] R. A. Dluhy, S. Shanmukh and S. Morita, *Surf. Interface Anal.* 2006, **38**, 1481.

[14] Y. Le Dréau, N. Dupuy, J. Artaud, D. Ollivier and J. Kister, *Talanta* 2009, **77**, 1748.

[15] B. Muik, B. Lendl, A. Molina-Diaz, M. Valcarcel and M. J. Ayora-Caňada, *Anal. Chim. Acta* 2007, **593**, 54.

[16] Y. le Dréau, N. Dupuy, V. Gaydou, J. Joachim and J. Kister, *Anal. Chim. Acta* 2009, **642**, 163.

[17] V. del Rĭo, M. P. Callao and M. S. Larrechi, *Internat. J. Anal. Chem.* 2011, 1.

[18] Y. B. Monakhova, A. M. Tsikin, S. P. Mushtakova and M. Mecozzi, *Microchem. J.* 2015, **118**, 211.

[19] M. Romeka, B. Gajda, E. Krzysztofowicz, M. Kepczynski and Z. Smorag, *Theriogenology* 2011, **75**, 42.

[20] A. B. Hendrich, O. Wesolowska, M. Komorowska, N. Motohashi and K. Michalak, *Biophys. Chem.* 2002, **98**, 275.

[21] P. L. Yeagle, *The Structure of Biological Membranes*, 3rd ed.; CRC

Press: Boca Raton, FL, USA, 2012.

[22] T. N. Bogatyrenko, E. B. Burlakowa and A. A. Konradov, *Proc. Int. Conf. Bioantioxidant* 1998, 26 (In Russian)

[23] E. M. Molochkina, I. B. Ozerowa, F. I. Braginskaya, O. M. Zorina and L. N. Shishkina, *Proc. Int. Conf. Bioantioxidant* 1998 153 (In Russian)

[24] N. M. Storozhok, M. G. Perevozkina, G. A. Nikiforov, *Russ. Chem. Biull. Int.ed.* 2005, **54**, 328.

[25] G. A. Nikiforov, I. S. Belostotskaya, V. B. Voleva, N. L. Komissarova and D. V. Gorbunov, *Tyumen Med. Acad. Sci. J.* 2003, **1**, 50.

[26] N. M. Storozhok, I. S. Belostotskaya, G. A. Nikiforov, I. F. Rusina and E. B. Burlakov, *Kinetics Catalysis* 2004, **45**, 813.

[27] J. H. Fendlez and E. J. Fendlez, *Catalysis in Micellar and Makromolecular Systems*, Academic, New York 1975, 290.

[28] Yu A. Ershov, V. A. Popkov and A. S. Berlyand, *General Chemistry, Biophysical Chemistry, Chemistry of Biogenic Elements, Nauka, Moscow* 1993, 560.

[29] K. Cieslik-Boczula, B. Czarnik-Matusewicz, M. Perevozkina, A. Filarowski, N. Boens, Wim M. De Borggraeve and A. Koll, *J. Mol. Struct.* 2008, **878**, 162.

[30] X. Bin, I. Zawisza, J. D. Goddard and J. Lipkowski, *Langmuir*, 2005, **21**, 330.

[31] J. Grdadolnik and D Hadži, *Spectrochim. Acta Part A* 1998, **54**, 1989.

[32] J. Jaumot, R. Gargallo, A. de Juan and R. Tauler, *Chemometr. Intell. Lab. Syst.* 2005, **76**, 101.

[33] K. Cieślik-Boczula, P. Świątek, A. Jaszczyszyn, P. Zawilska, K. Gąsiorowski, W. Malinka and G. Köhler, *J. Phys. Chem. B* 2014, **118**, 3605.

[34] T. Le Bihan and M. Pezolet, *Chem. Phys. Lipids* 1998, **94,** 13.

[35] Y. Inoko and T. Mitsui, *J. Phys. Soc. Jpn.* 1978, **44**, 1918.

[36] G. Cevc, *Biochim. Biphys. Acta* 1991, **1062**, 59.

[37] A. K. Riske, R. P. Barroso, C. C. Vequi-Suplicy, R. Germano, V. B. Henriques and M. T. Lamy, *Biochim. Biophys. Acta* 2009, **1788**, 954.

[38] R. N. Lewis, W. Pohle and R. N. McElhaney, *Biophys. J.* 1996, 70(6), 2736.

[39] D. G. Cameron, H. L. Casal and H. H. Mantsch, *Biochem.* 1980, **19**, 3665

[40] K. Ciesik, A. Koll and J. Grdadolnik, *Vib. Spectrosc*. 2006, **41**, 14.

Figure captions

Figure 1. The structure of ICPAN-C8.

Figure 2. EFA analyses of the high-frequency region (2970-2825 cm^{-1}), the low-frequency region (1505-940 cm^{-1}), and the whole-frequency region (2970-940 cm^{-1}) of the FTIR-ATR spectra of pure DPPC liposomes (A). Dashed lines – forward EFA analysis, solid line – backward EFA analysis. Concentration (B) and spectral profiles (C) of low- and high-temperature pure components (phase states) of DPPC liposomes, originated from the MCR-ALS analysis. $c_l^{wf}, c_l^{hf}, c_l^{lf}$ - concentration profiles of the low-temperature components derived from the MCR-ALS analysis of the high-, low-, and whole-frequency ranges, respectively; $c_h^{wf}, c_h^{hf}, c_h^{lf}$ - concentration profiles of the high-temperature components derived from the MCR-ALS analysis of the high-, low-, and whole-frequency ranges, respectively. Spectral profiles of the low-temperature phases – solid lines, spectral profiles of the high-temperature phases – dashed lines.

Figure 3. Concentration profiles determined by means of the MCR-ALS decomposition method of the low- and high-temperature pure components (phase states) in the DPPC liposomes. The MCR-ALS analyses were performed separately for the high- and low-frequency ranges of spectra, which were modulated by changes in their length, number or smoothing.

Figure 4. The pure spectral profiles of the low- and high-temperature pure components (phase states) present in pure DPPC liposomes during the heating. The MCR-ALS analyses were

performed separately for the high- and low-frequency ranges of spectra, which were modulated by changes in their length, number or smoothing.

Figure 5. Concentration profiles determined by means of the MCR-ALS decomposition method of the low- and high-temperature pure components (phase states) in the ICPAN-C8/DPPC system (A), ICPAN-C10/DPPC system (B), ICPAN-C12/DPPC system (C), and ICPAN-C16/DPPC system (D). c_l^{wf}, c_l^{hf}, c_l^{lf} - concentration profiles of the low-temperature components derived from the MCR-ALS analysis of the high-, low-, and whole-frequency ranges, respectively; c_h^{wf}, c_h^{hf}, c_h^{lf} - concentration profiles of the high-temperature components derived from the MCR-ALS analysis of the high-, low-, and whole-frequency ranges, respectively.

Figure 6. The pure spectral profiles (derived from MCR-ALS analysis) of the low- and high-temperature pure components (phase states) in pure DPPC liposomes – solid line, ICPAN-C8/DPPC system – dotted line, ICPAN-C10/DPPC system – dashed line, ICPAN-C12/DPPC system – dashed-one doted line, ICPAN-C16/DPPC system – dashed-two doted line.

Table 1. The maximum position and the half width of the $\nu_{as,s}(CH_2)$ bands from the high-frequency range of IR pure spectral profiles of the low- and high-temperature phase states in ICPAN/DPPC mixtures.

	$\nu_{as}(CH_2)$ / cm^{-1}		$\nu_s(CH_2)$ / cm^{-1}		$\nu_{1/2,s}(CH_2)$ / cm^{-1}		$\nu_{1/2,as}(CH_2)$ / cm^{-1}	
	At low temp.	At high temp.	At low temp.	At high temp.	At low temp.	At high temp.	At low temp.	At high temp.
DPPC	2917,3	2922,4	2849,7	2852,7	9,1	14,4	14,0	22,4
ICPAN-C8/DPPC	2916,8	2923,1	2849,8	2853,3	9,2	15,2	14,0	22,4
ICPAN-C10/DPPC	2917,3	2923,3	2850,0	2853,5	10,4	15,4	15,6	23,2
ICPAN-C12/DPPC	2918,9	2923,3	2850,6	2853,7	12,0	16,2	20,0	23,5
ICPAN-C16/DPPC	2917,3	2922,6	2849,9	2852,8	9,8	14,5	15,2	22,2

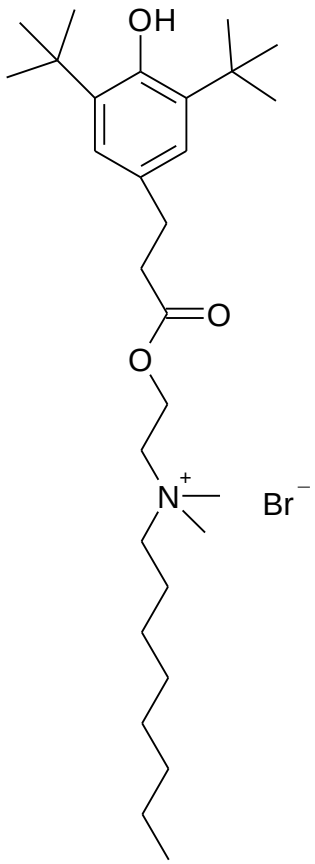

Figure 1

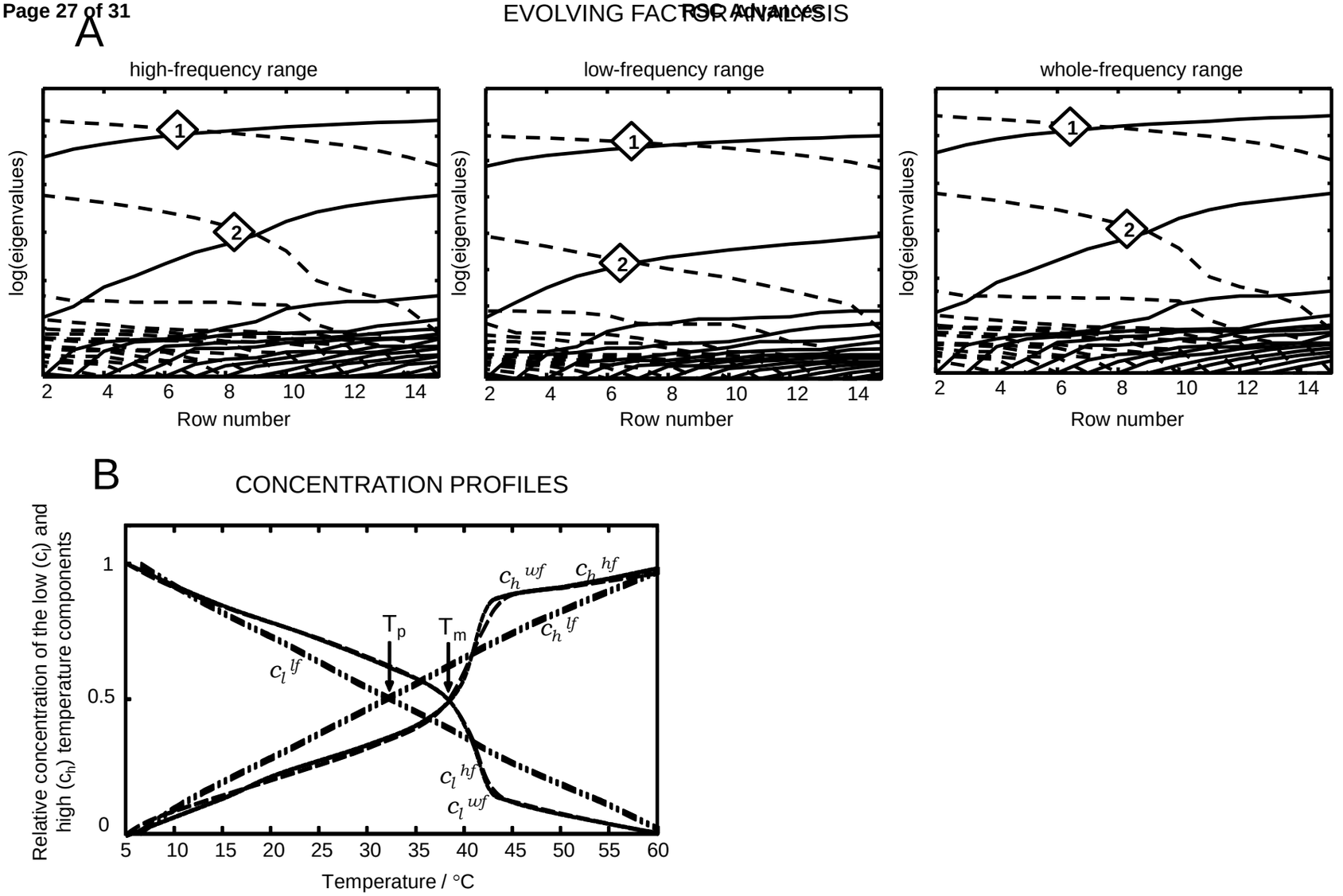

Figure 2

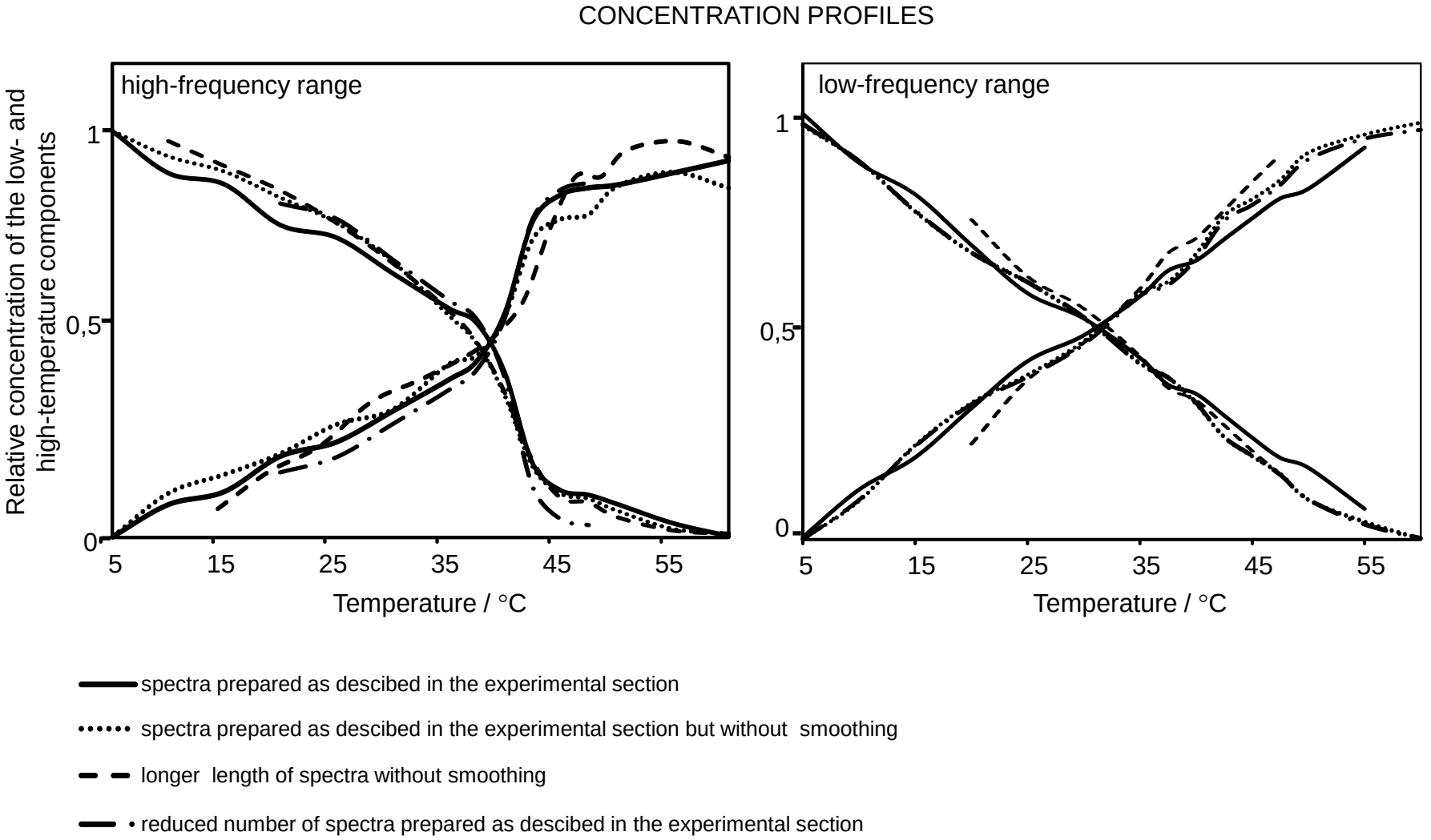

Figure 3

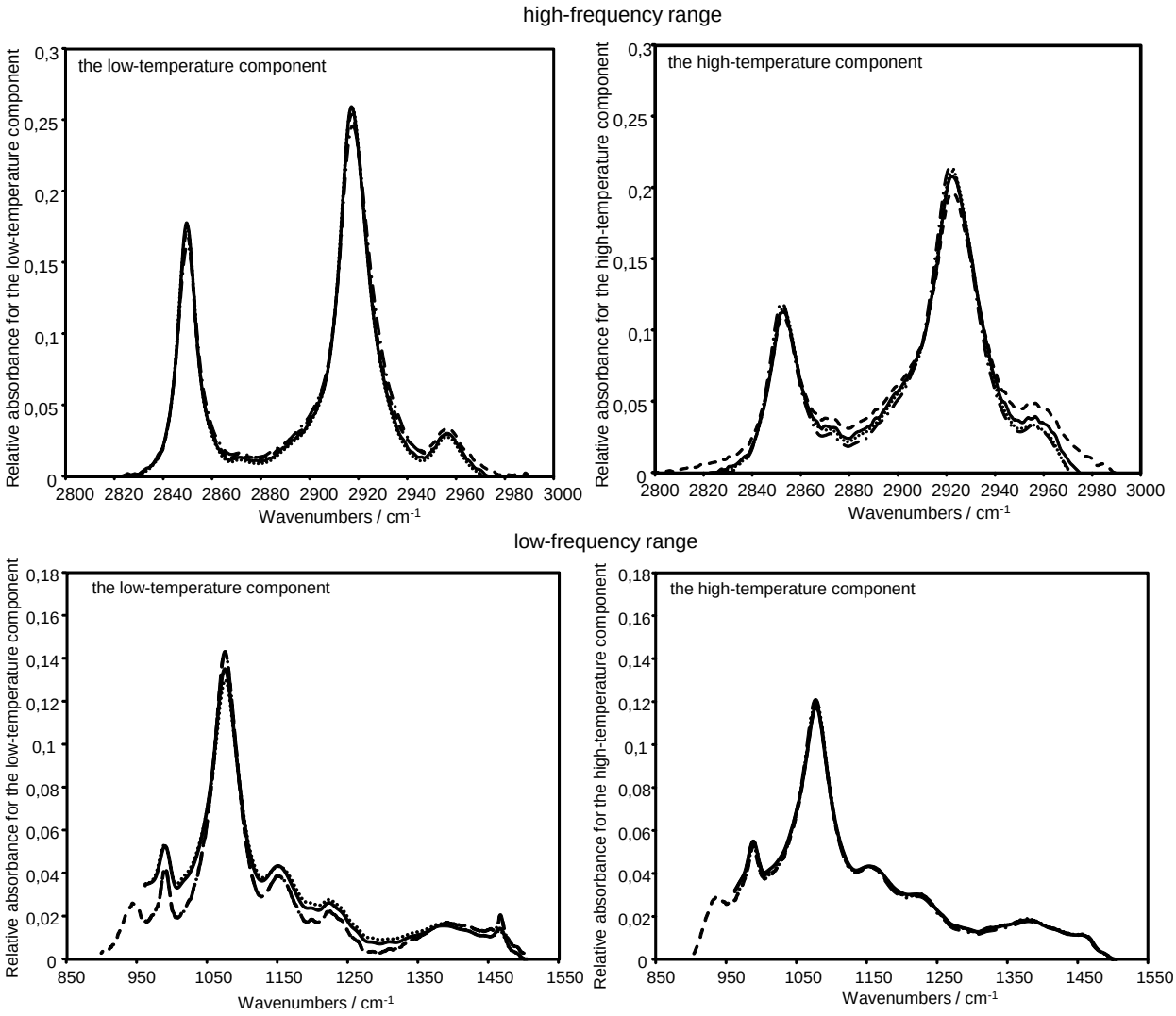

Figure 4

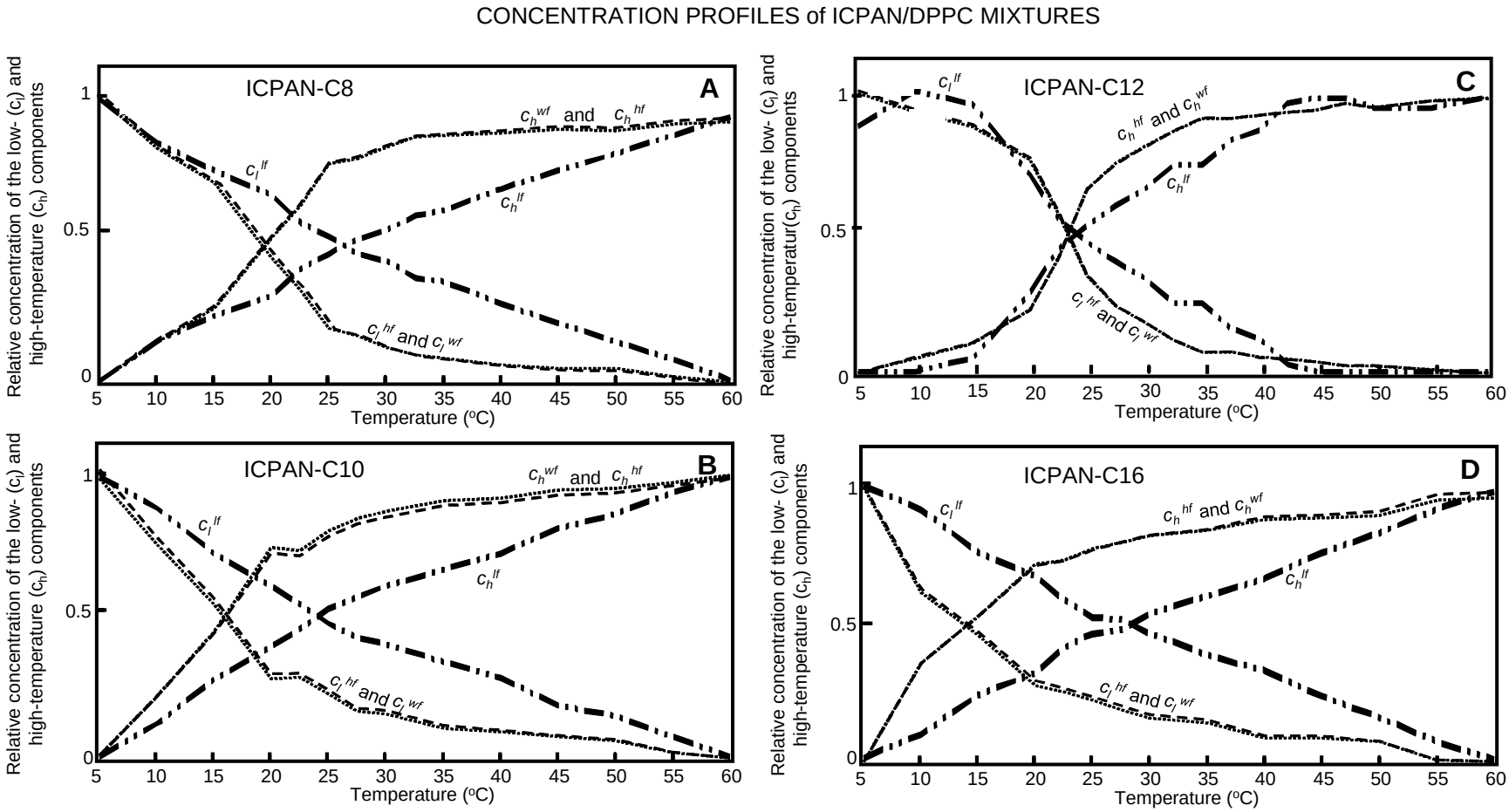

Figure 5

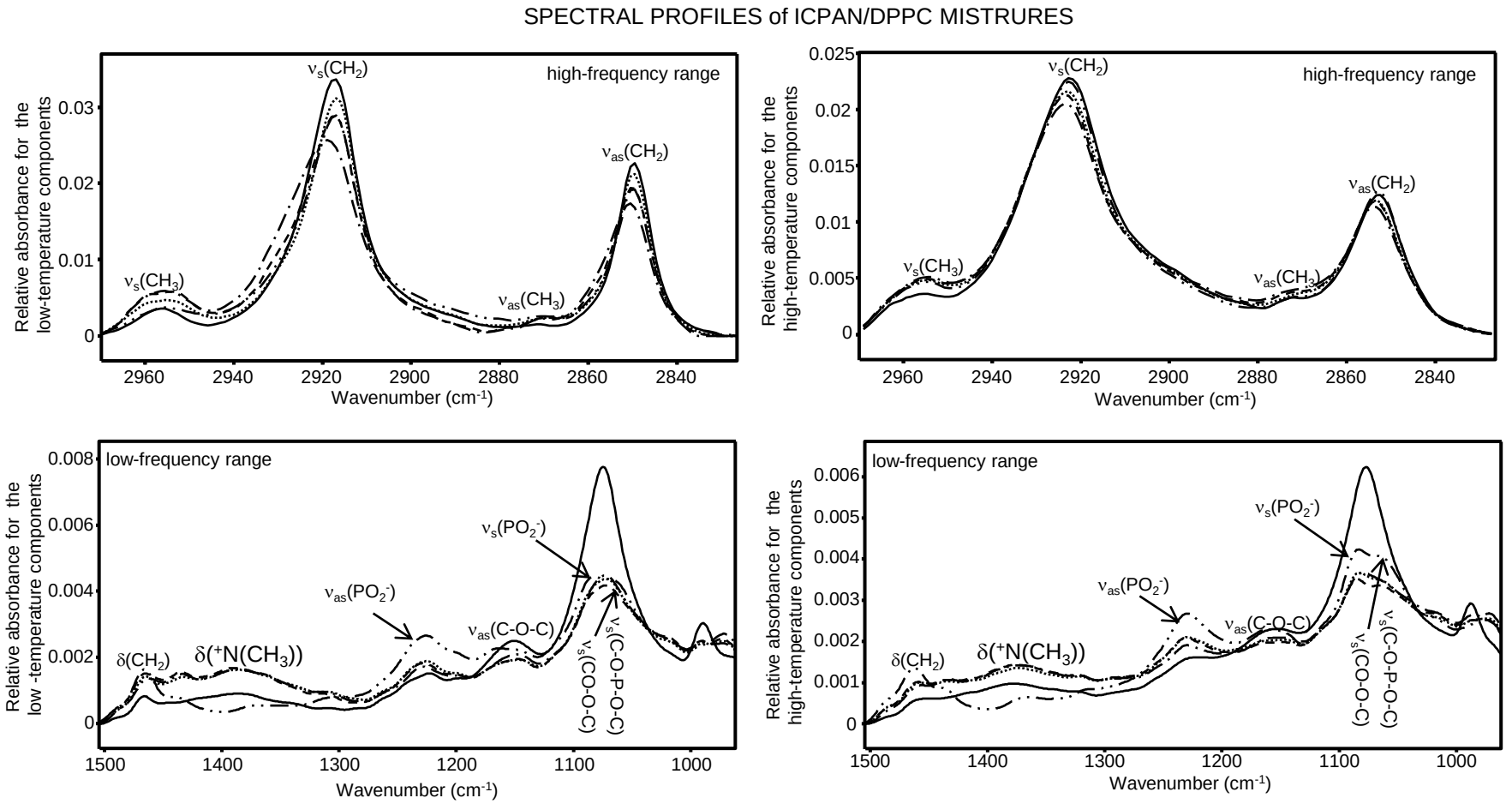

Figure 6